Received: Added at production | Revised: Added at production | Accepted: Added at production

DOI: xxx/xxxx

ARTICLE TYPE

Adaptive neural network control of robotic manipulators with input constraints and without velocity measurements

Heng Zhang[1] | Yangyang Zhao[1] | Yang Wang*[1] | Lin Liu[2]

[1]School of Information Science and Technology, ShanghaiTech University, Shanghai, China

[2]School of Advanced Manufacturing,, Sun Yat-sen University, Guangdong, China, Email: liulin67@mail.sysu.edu.cn

Correspondence

*Yang Wang, School of Information Science and Technology, ShanghaiTech University, Shanghai 201210, China. Email: wangyang4@shanghaitech.edu.cn

Funding Information

This work was supported in part by the Yangfan Program of Shanghai, China, under Grant 21YF142960.

Abstract

This paper addresses the trajectory tracking problem for a class of uncertain manipulator systems under the effect of external disturbances. The main challenges lie in the input constraints and the lack of measurements of joint velocities. We first utilize an extend-state-observer to estimate the velocity signals, then a neural-network-based adaptive controller is proposed to solve the problem, where a term based on the nominal model is included to enhance the tracking ability, and the effect of uncertainties and disturbances are compensated by a neural-network term. Compared with the existing methods, the main distinctive features of the presented approach are: i) The control law is guaranteed to be bounded by design, instead of directly bounded by a saturation function. ii) The trade-off between the performance and robustness of the presented controller can be easily tuned by a parameter that depends on the size of model uncertainties and external disturbances. By virtue of the Lyapunov theorem, the convergence properties of the proposed controller are rigorously proved. The performance of the controller is validated via both simulations and experiments conducted on a two-degree-of-freedom robot manipulator.

KEYWORDS:

Robotic manipulator, Adaptive control, Input saturation, Extend State Observer

1 | INTRODUCTION

Trajectory tracking control of robot manipulators has been extensively studied in past decades[1,2], but still a topic of both theoretical and practical significance, due to the dynamic couplings, model uncertainties, impact of external disturbances and input constraints, just to name a few. In the ideal case where the model and full-state of the system are available and accurate, adequate existing techniques[3,4], including the well-known PID control[5], are capable of achieving asymptotic tracking objectives with satisfactory transient performance. However, in practical applications, the uncertainties of the model are almost inevitable, especially considering the wear-out, and an environment without noise is not realistic either.

Numerous methods[6,7,8] have been developed to address the challenge stemming from the model uncertainties and external disturbances, which are usually termed as "lumped uncertainties" in the literature[9]. Among them, the neural-network-based (NN-based) adaptive control attracts plenty of attention[10,11] as the adaptive methodology[12] is able to adjust the controller parameters on-line to cope with the lumped uncertainties, while the NN-based mechanisms[13] is capable of approximating the nonlinear dynamics in a linear manner. One can even avoid the use of the robot dynamic model[14] by means of employing a pure NN-based controller. However, it is practically illogical to totally ignore the physical model because, in most cases, certain (structural)

prior knowledge of the manipulator to be controlled is indeed trivial to obtain. Therefore, the control problem addressed in this paper considers the nominal model to be largely uncertain, but not completely unknown.

Despite the intriguing performance of aforementioned adaptive NN methods, the constraints of actuators are rarely considered, which, if not properly coped, may severely degrade system performances and even cause instability [15,16]. The controllers proposed in [17,18] are bounded, but the boundary of the control signal cannot be determined by the users, that is, whether this bounded input satisfies the limits of the actuator or not, is unknown and unmodifiable [19]. It is of practical importance to constrain the control signal within the physical limits before it is sent to the actuator. An intuitive solution is to apply a sigmoid function to the control law, as [15] did. However, in this way, certain sacrifices of performance are inevitable, especially when the control signals are kept saturated during the whole transient period. The controller proposed in [20] have adjustable boundaries, but it also require an accurate model. In [21], a control algorithm based on prescribed performance control method is proposed to address the tracking problem under different input constraints. However, it requires the utilization of fuzzy control to model system uncertainties, rendering the controller complex.

Moreover, the majority control methods mentioned above assume that the full-state of the system can be measured directly and accurately. However, in practice, not all the states of the manipulator can be obtained directly [22]. As the tracking objective is in generally specified in terms of the angular position, this work focuses on the situation where the velocity measurements of the robotic manipulator are unavailable [23]. On the one hand, as shown in [24,25], the information on the joint velocity is essential to construct a stabilizing controller. On the other hand, the joint velocity can not be obtained by differentiating the angular data due to the sensor noise [26]. Hence, designing an effective observer to recover the velocity information becomes another attractive research topic [27] in the manipulator control problem. But how to combine such an observer with a stabilizing adaptive controller that satisfies the input constraints and achieves the asymptotic tracking of desired trajectories remains an issue far from settled, which is therefore the topic of this paper.

Based on the preliminary work [28], this paper continues the quest of designing a novel NN-based adaptive controller for uncertain robotic manipulator systems under the input constraint, the external disturbances, and more importantly, the hypothesis that the joint velocity signals are unavailable. The main obstacle of solving this problem lies in the fact that the stability of the closed-loop system relies on the accurate velocity estimates, while the convergence of estimation error in general needs the trajectories of the closed-loop system to be bounded, i.e., the system has been stabilized. Not to mention, we also need to consider the input constraints. To address these issues, inspired by the Extended State Observer (ESO) [29], a modified fal-based ESO is constructed to provide the estimate of angular velocity while avoiding excessive initial errors. Then, the observer errors were added to the lumped uncertainties to be compensated by a neural network. Next, projection operations are adopted for the NN and observer in order to construct a stabilizing and bounded control law. Further, a $\tanh()$ function is utilized here instead of using directly the saturation function to allow the boundary of the input signal to be rendered verifying the limits of actuators.

In summary, the proposed neural network-based adaptive controller is a tunable combination of model-based control and data-driven learning mechanisms. By introducing the parameter ι to adjust the algorithm's confidence in the model, we enable the proposed approach to switch and balance between robustness and performance. Furthermore, in contrast to existing literature [15,30], the controller presented in this paper naturally adheres to input constraints. Unlike methods that directly restrict the maximum controller signal using sigmoid saturation functions or physical constraints, our controller, while satisfying the constraints, does not compromise control performance, and it does not induce system instability. Additionally, the boundaries of the controller output signals are fully adjustable, allowing our controller to adapt better to a wider range of application scenarios.

The rest of the paper is organized as follows. In section 2, some knowledge about preliminaries is introduced, and the dynamic model of system and control problem concerned are formally stated. A velocity observer whose estimation error is always bounded is introduced in section 3. By using the theoretical results of section 3, a new NN-based adaptive controller is proposed in section 4 to solve the problem. Then, in section 5, we present a rigorous analysis to show the ISS property of the closed-loop system and the boundedness of the input signal. Finally, simulation results and experiments are given in section 6 and 7, respectively. A brief remark is concluded in section 8, and the appendix provides some supporting proofs.

2 | PROBLEM FORMULATION

2.1 | Preliminaries

The NN is an efficient tool to approximate unknown nonlinear functions. In this paper, the model uncertainties and external disturbances are formulated as a smooth function $f(\cdot) : \mathbb{R}^m \to \mathbb{R}^n$ over a compact set $\Omega_N \subseteq \mathbb{R}^m$, and approximated as[31]:

$$\hat{f}(z) \triangleq \hat{W}^\top \sigma(z) \tag{1}$$

where $z \in \mathbb{R}^m$ is the input vector, $\hat{W} \in \mathbb{R}^{\mathcal{L}\times n}$ is the weight matrix with $\mathcal{L}$ denoting the number of neurons, and $\sigma(z) \in \mathbb{R}^{\mathcal{L}}$ is the Gaussian activation function defined as $\sigma(z) \triangleq [\sigma(z) \cdots \sigma_{\mathcal{L}}(z)]^\top$ with the basis Gaussian functions $\sigma_i(\cdot)$, for $i = 1, 2, \cdots, \mathcal{L}$, given by $\sigma_i(z) \triangleq \prod_{k=1}^{m} e^{-(z_k-\mu_{ik})^2/2p_{ik}}$ in which z_k, μ_{ik} and p_{ik} are, respectively, the k-th components of z, the mean vector $\mu_i \in \mathbb{R}^m$, and the corresponding variance $p_{ik} \in \mathbb{R}$. Because of the nature of the Gaussian function, it is obvious that $\sigma(z)$ is bounded, e.g. $||\sigma(z)|| \leq \zeta_\sigma$. On the other hand, according to[17], any smooth function $f(\cdot)$ over the set Ω_N can be represented by

$$f(z) = W^\top \sigma(z) + \epsilon(z) \tag{2}$$

where $\epsilon(z) \in \mathbb{R}^n$ is a bounded functional reconstruction error, and $W \in \mathbb{R}^{\mathcal{L}\times n}$ is a bounded constant ideal weight matrix.

Property 1. For any smooth function $f(z)$, with a fixed number of neurons, there exists an ideal weight matrix W, to make the approximation error equal to the structural error, such that the following bound can be considered over the compact set Ω_N [32]

$$||W||_F^2 = tr(W^\top W) \leq W_B, \quad ||\epsilon(z)|| \leq \epsilon_N$$

where W_B, $\epsilon_N \in \mathbb{R}^+$ are positive constants. ◁

From (1) and (2), the function approximation error can be written as

$$f - \hat{f} = \tilde{W}^\top \sigma(z) + \epsilon(z) \tag{3}$$

where $\tilde{W}(t) \in \mathbb{R}^{\mathcal{L}\times n}$, defined as $\tilde{W} \triangleq W - \hat{W}$, denotes the estimate mismatch for the ideal weight matrix.

In this paper, the Euclidean norm of a vector $x \in \mathbb{R}^n$ is denoted by $\|x\| = \sqrt{\sum_{i=1}^{n} x_i^2}$. $\mathbb{R}^+$ denotes the positive real values. For a matrix $A \in \mathbb{R}^{n\times n}$, $\lambda_{\min}(A)$ and $\lambda_{\max}(A)$, respectively, denote the minimum and maximum eigenvalues of A. $||A|| = \sqrt{\lambda_{\max}(A^\top A)}$ is the induced norm, $||A||_F$ is the Frobenius norm (F-norm), and $tr(A)$ denotes the trace of A. $\mathcal{C}^n$ represents a class of functions or mappings that are n times differentiable. $\nabla(\cdot)$ denotes the gradient of the function with respect to its argument.

2.2 | Problem Formulation

An n-link robotic manipulator modeled by the following Euler-Lagrange equation[33] is considered:

$$M(q)\ddot{q} + C(q, \dot{q})\dot{q} + F(\dot{q}) + G(q) + T_d = \tau \tag{4}$$

where $q = [q_1, q_2, \cdots, q_n]^\top, \dot{q} = [\dot{q}_1, \dot{q}_2, \cdots, \dot{q}_n]^\top, \ddot{q} = [\ddot{q}_1, \ddot{q}_2, \cdots, \ddot{q}_n]^\top \in \mathbb{R}^n$ are, respectively, the vectors of angular position, velocity, and acceleration of joints with $q(t)$ being the only states that are available for measurement; $M(q) \in \mathbb{R}^{n\times n}$ represents the inertia matrix; $C(q, \dot{q}) \in \mathbb{R}^{n\times n}$ is the centrifugal-Coriolis matrix; $G(q) \in \mathbb{R}^n$ denotes the gravity vector; $F(\dot{q}) \in \mathbb{R}^n$ is the friction vector; $T_d \in \mathbb{R}^n$ and $\tau \in \mathbb{R}^n$ represent the external disturbances and the output torque of actuator, respectively.

This work addresses the trajectory tracking problem for systems (4) under input constraints, the influence of model uncertainties and external disturbances. To be more specific, the control objective is to steer the position and velocity of each joint of the manipulator to follow a certain given time-dependent C^2 function $q_d(t)$, given only the measurement of q and nominal model denoted by $M_o(q)$, $C_o(q, \dot{q})$, $F_o(\dot{q})$, $G_o(q)$. Obviously, taking into account the limited actuator torque, the manipulator system is only able to track a certain type of desired trajectory and handle bounded disturbances and model uncertainties.

The input constraints are given in the context of the limitation of the angular velocity and the norm-bound of the actuator torque and verify the following assumptions.

Assumption 1. The limitations of the angular and angular velocity of the manipulator joints are known and given in the form of:

$$\beta_q \triangleq \max_{i\in I_n} \sup_{t\geq 0}\{q_i(t)\} \in \mathbb{R}^+, \quad \beta \triangleq \max_{i\in I_n} \sup_{t\geq 0}\{\dot{q}_i(t)\} \in \mathbb{R}^+, \quad I_n \triangleq \{1, \cdots, n\}$$ ◁

Remark 1. In practical applications, the upper bound of the angle q_i is determined by the mechanical design, and q_i can always be expressed as the value of $[-\pi, \pi]$ rad. On the other hand, the angular velocity $\dot{q}_i$ is bounded by the power of the motor[34].

For specific manipulator systems, such as the Kinova selected in this paper, its parameters can be obtained from the official configuration as $\beta_q = \pi$ rad and $\beta = 0.2\pi$ rad/s. These two types of variables are trivial to obtain and exist for all practical manipulator systems.

Without loss of generality, the mismatches between the true plant and the nominal model are represented by $\Delta M(q)$, $\Delta C(q,\dot{q})$, $\Delta F(\dot{q})$, $\Delta G(q)$ which are assumed to be additive, namely verifying the following relations:

$$M_o(q) \triangleq M(q) + \Delta M(q), \quad C_o(q,\dot{q}) \triangleq C(q,\dot{q}) + \Delta C(q,\dot{q}), \quad F_o(\dot{q}) \triangleq F(\dot{q}) + \Delta F(\dot{q}), \quad G_o(q) \triangleq G(q) + \Delta G(q) \tag{5}$$

and bounded. The boundary of parametric uncertainties will be clarified later.

As for the external disturbances T_d, it is assumed that:

Assumption 2. The external disturbances T_d and its time derivative $\dot{T}_d$ are both norm-bounded and verified by $\sup_{t\geq 0}\|T_d\| \leq \zeta_d$ for some positive constant ζ_d known a prior. ◁

Substituting (5) into (4), the dynamics model is rewritten as:

$$M_o(q)\ddot{q} + C_o(q,\dot{q})\dot{q} + F_o(\dot{q}) + G_o(q) = \tau + \delta \tag{6}$$

where $\delta := \Delta M(q)\ddot{q} + \Delta C(q,\dot{q})\dot{q} + \Delta F(\dot{q}) + \Delta G(q) - T_d$ stands for the total effect of uncertainties and external disturbances, usually termed as "lumped uncertainties" in the literature. The desired trajectory $q_d(t) = [q_{d1}(t), \cdots, q_{dn}(t)]^\top \in \mathbb{R}^n$ is determined by users, satisfying that $\sup_{t\geq 0}||Q_d(t)|| = \zeta_q$ with $Q_d(t) = [q_d^\top, \dot{q}_d^\top, \ddot{q}_d^\top, \dddot{q}_d^\top]^\top \in \mathbb{R}^{4n}$ and positive constant ζ_q. Let positive constant vector $B_v = [B_{v1}, \cdots, B_{vn}]^\top \in \mathbb{R}^n$, $B_a = [B_{a1}, \cdots, B_{an}]^\top \in \mathbb{R}^n$ denote the upper bounds of $\dot{q}_d(t)$ and $\ddot{q}_d(t)$ as

$$B_{vi} \triangleq \sup_{t\geq 0}||\dot{q}_{di}(t)||, \quad B_{ai} \triangleq \sup_{t\geq 0}||\ddot{q}_{di}(t)||, \quad \forall i \in I_n \tag{7}$$

It is reasonable to require that B_v should satisfy $\|B_v\| \leq \sqrt{n}\beta$, in which β represents the physical limitation of the actuator that is defined in the Assumption 1.

Below we listed a few properties[4] of manipulator systems that are widely recognized and fundamental for the subsequent design and analysis.

Property 2. For all $x \in \mathbb{R}^n$, the time derivative of inertia matrix $M(q)$ and the centrifugal-Coriolis matrix $C(q,\dot{q})$ satisfy the following skew-symmetric relationship:

$$x^\top(\dot{M}(q) - 2C(q,\dot{q}))x = 0$$ ◁

Property 3. The positive-definite symmetric inertia matrix $M(q)$, the centrifugal-coriolis matrix $C(q,\dot{q})$, the friction $F(\dot{q})$ and gravitational vector $G(q)$ satisfy the following inequalities:

$$\underline{m}||x||^2 \leq x^\top M(q)x \leq \overline{m}||x||^2, \quad ||C(q,\dot{q})|| \leq \zeta_c||\dot{q}||, \quad ||F(\dot{q})|| \leq \zeta_{f_d}||\dot{q}|| + \zeta_{f_s}, \quad ||G(q)|| \leq \zeta_g, \quad \forall x \in \mathbb{R}^n \tag{8}$$

for some known constants $\zeta_c, \zeta_{f_d}, \zeta_{f_s}, \zeta_g \in \mathbb{R}^+$, and $\underline{m}, \overline{m} \in \mathbb{R}^+$ are respectively defined as

$$\underline{m} \triangleq \min_{\forall q\in\mathbb{R}^n} \lambda_{min}(M), \quad \overline{m} \triangleq \max_{\forall q\in\mathbb{R}^n} \lambda_{max}(M).$$ ◁

In this paper, we propose a novel robust feedback controller

$$\tau(t) \triangleq [\tau_1, \cdots, \tau_n] \in \mathbb{R}^n$$

that simultaneously tackles three major challenges, namely the effect of "lumped uncertainties", input constraint and the immeasurable angular velocity. To the best of our knowledge, this paper is the first one that takes into account for all these difficulties at the same time, regardless of the intensive study of the control problem of Euler-Lagrange system.

Define $e(t) \triangleq q(t) - q_d(t)$, $\dot{e}(t) \triangleq \dot{q}(t) - \dot{q}_d(t)$ and $\ddot{e}(t) \triangleq \ddot{q}(t) - \ddot{q}_d(t)$ to denote the error signals, $\tau_N \in \mathbb{R}$ to represent the upper-bound of the torque of the actuator. Note that, since $\dot{q}(t)$ is immeasurable under the setting of this paper, the only available error signal for feedback is $e(t)$. Now, the problem considered in this paper is formally stated as follows:

Problem 1. Suppose Assumptions 1-2 hold, given only angular position $q(t)$, design a dynamic feedback controller $\tau = [\tau_1, \cdots, \tau_n]^\top \in \mathbb{R}^n$ for System (4) such that the output of the controller are bounded by the limits of actuators, i.e.

$$|\tau_i(t)| \leq \tau_N, \quad \forall i \in I_n$$

for all $t \geq 0$, and the tracking errors of the closed-loop system asymptotically convergent to a ball-neighborhood of the origin whose radius depends on the size of "lumped uncertainties", that is

$$\lim_{t\to\infty} e_i(t) \leq \bar{\alpha}_i(\Delta f_i), \quad \lim_{t\to\infty} \dot{e}_i(t) \leq \bar{\beta}_i(\Delta f_i), \quad \forall i \in I_n \tag{9}$$

for some class-$\mathcal{K}$ functions $\bar{\alpha}_i(\cdot)$ and $\bar{\beta}_i(\cdot)$, where Δf_i is the i-th element of $\Delta f = [\Delta f_1, \cdots, \Delta f_n]^\top \in \mathbb{R}^n$ defined in (28). ◁

Remark 2. It's worth pointing out that, different from the existing methods in the literature, here we do not bound the input by a saturation function. Instead, by appropriate choice of the tuning gains, the proposed algorithm guarantees that the control input will not exceed the boundary τ_N. In this way, the performance of the system will not degrade in practical implementation. Furthermore, the proposed scheme provides some insights into the performance limitation of the system.

3 | OBSERVER DESIGN

In this section, an extended state observer[35] is designed to obtain the estimate of angular velocity, which is not available for direct measurement. The results in this section will serve as a building block for the analysis and design of the NN-based adaptive controller of the next section.

First, introducing $x_{i1} \triangleq q_i$, $x_{i2} \triangleq \dot{q}_i$ and denoting T_i the i-th row of the matrix $M_o(X_1)^{-1}$ as follows

$$q \triangleq [x_{11}, x_{21}, \cdots, x_{n1}]^\top = X_1 \in \mathbb{R}^n, \quad \dot{q} \triangleq [x_{12}, x_{22}, \cdots, x_{n2}]^\top = X_2 \in \mathbb{R}^n, \quad M_o(X_1)^{-1} \triangleq [T_1^\top, \cdots, T_n^\top]^\top = T \in \mathbb{R}^{n\times n} \tag{10}$$

dynamics (6) can be recast as n coupled second-order subsystems whose dynamic is governed by

$$\begin{aligned} \dot{x}_{i1} &= x_{i2}, \quad x_{i1}(0) = q_i(0) \\ \dot{x}_{i2} &= B_f x_{i3} + T_i[\tau - G_o(X_1)], \quad x_{i2}(0) = \dot{q}_i(0) \end{aligned} \tag{11}$$

where x_{i3} is a normalized extended state containing all the decoupled terms and lumped uncertainties defined as

$$x_{i3} = \frac{1}{B_f} T_i[-C_o(X_1, X_2)X_2 - F_o(X_2) + \delta] \tag{12}$$

where $B_f \triangleq \max_{i\in I_n} \sup_{t\geq 0} T_i[-C_o(X_1, X_2)X_2 - F_o(X_2) + \delta]$. Clearly, $|x_{i3}| \in [0, 1)$.

Remark 3. A conservative value of B_f can be easily obtained by finding the upper-bounded of term T_i, C_o, X_2, $F_o(X_2)$ and δ according to Assumption 1, 2 and Property 3, respectively.

Use $\hat{x}_i \triangleq [\hat{x}_{i1}, \hat{x}_{i2}, \hat{x}_{i3}]^\top$ to denote the estimate $x_i \triangleq [x_{i1}, x_{i2}, x_{i3}]^\top$, an ESO[35] for i-th subsystem defined in (11) is designed as

$$\begin{aligned} \dot{\hat{x}}_{i1} &= \hat{x}_{i2} + \frac{k_{i1}}{l} g_1(l^2(x_{i1} - \hat{x}_{i1})) \\ \dot{\hat{x}}_{i2} &= B_f \hat{x}_{i3} + T_i[\tau - G_o(X_1)] + k_{i2} g_2(l^2(x_{i1} - \hat{x}_{i1})) \\ \dot{\hat{x}}_{i3} &= \frac{1}{B_f} k_{i3} l g_3(l^2(x_{i1} - \hat{x}_{i1})) \end{aligned} \tag{13}$$

with constant gain $l \in \mathbb{R}$, and the state initialization $\hat{x}_i(0)$ of observer expected to be inside a hyper-sphere of origin.

If no knowledge of the observer state is available, the best choice for initialization is zero. However, if a priori estimation is possible, we may set the initial values for $\hat{x}_i$ to be those estimates for improved performance.

In addition, $g_j(\nu) : \mathbb{R} \to \mathbb{R}$ is a nonlinear function[29] constructed as

$$g_j(\nu) = \begin{cases} \nu, & |\nu| \leq 1 \\ |\nu|^{\theta_j} \text{sign}(\nu), & |\nu| \geq 1 \end{cases} \tag{14}$$

where $\theta_j = j\theta - (j-1)$, $j \in \{1, 2, 3\}$. θ and l are tuning gains to be determined later. k_{ij}, $i \in I_n$, $j \in \{1, 2, 3\}$, are constants chosen such that the following matrix

$$K_i = \begin{pmatrix} -k_{i1} & 1 & 0 \\ -k_{i2} & 0 & 1 \\ -B_f k_{i3} & 0 & 0 \end{pmatrix} \in \mathbb{R}^{3\times 3} \tag{15}$$

is Hurwitz.

Considering the constraints of inputs, it is essential to ensure the boundedness of the state of the observer (13) since it will be employed in the subsequent design of the controller. Therefore, we impose a projection operator on the state $\hat{x}_i$ as follows:

$$Pr(\dot{\hat{x}}_i) = \begin{cases} \dot{\hat{x}}_i, & \text{if} \|\Lambda\hat{x}_i\| < S_i \text{ or} \\ & \|\Lambda\hat{x}_i\| = S_i \text{ and } \dot{\hat{x}}_i^\top \Lambda^\top \Lambda \hat{x}_i \le 0 \\ \dot{\hat{x}}_i - \frac{\Lambda^\top \Lambda \hat{x}_i \hat{x}_i^\top \Lambda^\top \Lambda}{\hat{x}_i^\top \Lambda^\top \Lambda \Lambda^\top \Lambda \hat{x}_i} \dot{\hat{x}}_i, & \text{otherwise} \end{cases} \tag{16}$$

where $\Lambda \in \mathbb{R}^{3\times3}$ is defined as $\Lambda^\top\Lambda \triangleq L^{-1}P_i^{-1}L^{-1}$, with L and P_i are symmetric positive definite matrix defined in (A2) and (A5), respectively. S_i denotes a hyper-sphere inside which we aim to keep the trajectory of the observer, assuming the initial condition of the observer is inside it.

Remark 4. Thanks to the physical boundary of $q(t)$, the boundaries of $\dot{q}(t)$ provided in the Assumption 1, and re-scaled operation imposed on x_{i3}, it is easy to find a conservative value of S_i, for instance

$$S_i = \|\Lambda\|\sqrt{\beta_q^2 + \beta^2 + 1} \tag{17}$$

Remark 5. For the convenience of showing the error convergence of the observer, we use the standard projection operator[36] with little modification, but it has the same functionality as the standard one, i.e., variables are limited by the prescribed bounds. The proof is given in Appendix A.1.

Define the estimation error as $\tilde{x}_{i1} \triangleq x_{i1}(t) - \hat{x}_{i1}(t)$, $\tilde{x}_{i2} \triangleq x_{i2}(t) - \hat{x}_{i2}(t)$, with $i \in I_n$. The convergence property guaranteed by the Observer (13) is summarized in the next Theorem 1.

Theorem 1. Suppose Assumption 2 holds, consider Subsystem (11) as well as the Observer (13) and (16), there exist $\epsilon_\theta \in (0,1)$ and $l^* > 0$ such that for any $\theta \in [1-\epsilon_\theta, 1+\epsilon_\theta]$, $l \in [l^*, \infty)$, the estimation errors $\tilde{x}_{i1}(t)$ and $\tilde{x}_{i2}(t)$ will asymptotically converge to the neighborhood of origin, i.e.

$$\lim_{t\to\infty} |\tilde{x}_{i1}| \le \kappa_i(\delta, l), \quad \lim_{t\to\infty} |\tilde{x}_{i2}| \le \bar{\kappa}_i(\delta, l), \quad \forall i \in I_n \tag{18}$$

where $\kappa_i(\cdot,\cdot)$ and $\bar{\kappa}_i(\cdot,\cdot)$ are some class $\mathcal{KL}$ functions[1] , and δ is the lumped uncertainty, consisting of model uncertainties and external disturbances, defined in (6). ◁

The proof of Theorem 1 is presented in Appendix A.1.

4 | NEURAL NETWORK-BASED ADAPTIVE CONTROLLER

Utilizing the estimate of the angular velocity $\dot{q}$ in Section 3, an NN-based adaptive controller is finally proposed to achieve trajectory tracking. Detailed block diagram of the proposed control scheme is shown in Fig. 1. As we are about to demonstrate, the control algorithm is feasible and capable of addressing Problem 1.

In view of (11), the vector of estimation error can be defined as

$$\tilde{X}_1 \triangleq X_1 - \hat{X}_1 = [\tilde{x}_{11}, \tilde{x}_{12}, \cdots, \tilde{x}_{1n}]^\top, \quad \dot{\tilde{X}}_1 = \tilde{X}_2 \triangleq X_2 - \hat{X}_2 = [\tilde{x}_{21}, \tilde{x}_{22}, \cdots, \tilde{x}_{2n}]^\top, \tag{19}$$

and $\hat{e} := \hat{X}_1 - q_d$, $\dot{\hat{e}} := \dot{\hat{X}}_1 - \dot{q}_d$. We start by introducing two auxiliary signals as follows:

$$r = \dot{\hat{e}} + \frac{\alpha}{1+\beta'}\text{Tanh}(e) + \alpha\chi(e) \tag{20}$$

$$\dot{\chi} = -K_1 r - K_2\chi + \alpha\text{Tanh}(e), \quad \chi(0) = 0 \tag{21}$$

where $\alpha \in \mathbb{R}^+$ is a constant tuning gain, $K_1, K_2 \in \mathbb{R}^{n\times n}$ are diagonal positive-definite gain matrices, $\beta' \triangleq 2\beta \ge \max_{i\in I_n} ||\dot{e}_i||$ denotes the upper bound of the tracking error of angular velocity, and the bounded vector function $\text{Tanh}(\cdot) : \mathbb{R}^n \to \mathbb{R}^n$ is defined as $\text{Tanh}(v) \triangleq [\tanh(v_1), \cdots, \tanh(v_n)]^\top$ for any n-dimensional vector v.

Designing auxiliary signals r and χ serves the purpose of enabling our proposed controller to naturally meet input constraint requirements and facilitate stability analysis. The function of these auxiliary signals is to ensure that the controller's output signals are subject to soft constraints, thereby guaranteeing that the predefined input constraints are not violated.

[1] A NL class function $f(x,y) : \mathbb{R}\times\mathbb{R} \to \mathbb{R}^+$ is defined as the function satisfying as follows conditions: i): while y is fixed, $f(x,y)$ increases as x increasing; ii): while x is fixed, $f(x,y)$ decreases as y increasing; iii): $f(0,y) > 0$.

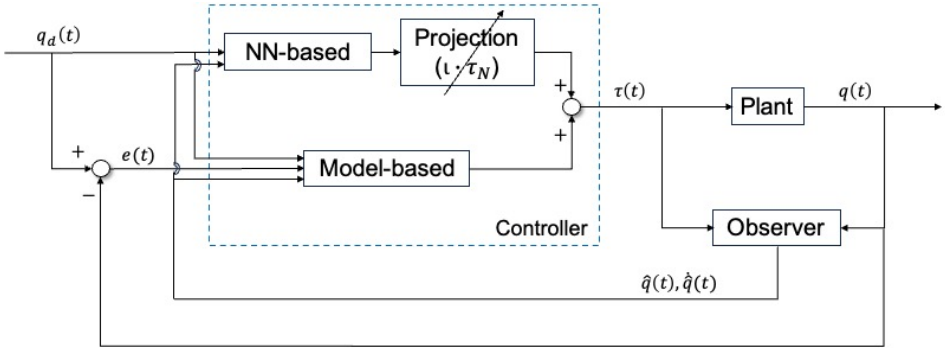

FIGURE 1 The block diagram of the NN-based adaptive controller.

Thanks to the fact that $\hat{e} = e - \tilde{X}_1$, we have that the dynamic of r is governed by

$$\dot{r} = \ddot{e} - \ddot{\tilde{X}}_1 + \frac{\alpha}{1+\beta'}\mathrm{Cosh}^{-2}(e)\cdot\dot{e} - \alpha K_1 r - \alpha K_2 \chi + \alpha^2 \mathrm{Tanh}(e) \tag{22}$$

where the matrix function $\mathrm{Cosh}(\cdot) : \mathbb{R}^n \to \mathbb{R}^{n\times n}$ is defined as $\mathrm{Cosh}(x) \triangleq \mathrm{diag}\{\cosh(x_1), \cdots, \cosh(x_n)\}$ for any n-dimensional vector x. Now, subtracting $M(q)\ddot{q}_d$ from both sides of (4), we have

$$M(q)\ddot{e} = \tau - C(q,\dot{q})\dot{q} - F(\dot{q}) - G(q) - T_d - M(q)\ddot{q}_d \tag{23}$$

Then, we substitute (22) into (23) to eliminate $\ddot{e}$ and rewrite the dynamic equation in terms of the auxiliary signal r as

$$M(q)\dot{r} = -C(q,\dot{q})r - \alpha M(q)K_1 r - T_d + \tau + h \tag{24}$$

where we have replaced $C(q,\dot{q})q$ with $C(q,\dot{q})r$ and put the rest of terms into the variable h, defined by

$$h \triangleq M(q)[\frac{\alpha}{1+\beta'}\mathrm{Cosh}^{-2}(e)\dot{e} - \alpha K_2\chi + \alpha^2\mathrm{Tanh}(e) - \ddot{q}_d - \ddot{\tilde{X}}_1] + C(q,\dot{q})(r-\dot{q}) - F(\dot{q}) - G(q) \tag{25}$$

Next, after some calculations, we split h into two parts (one part is known while the other collects the effect of parametric uncertainties and estimation error, which will be compensated by an adaptive NN-based term), that is $h := \hat{h} + \tilde{h}$, and $\hat{h}$ and $\tilde{h}$ are given, respectively, by

$$\hat{h} = M_o(q_d)[\frac{\alpha}{1+\beta'}\mathrm{Cosh}^{-2}(e)\dot{\hat{e}} - \alpha K_2\chi + \alpha^2\mathrm{Tanh}(e) - \ddot{q}_d] + C_o(q_d,\dot{q}_d)[-\dot{q}_d + \frac{\alpha}{1+\beta'}\mathrm{Tanh}(e) + \alpha\chi] - F_o(\dot{q}_d) - G_o(q_d) \tag{26}$$

and

$$\begin{aligned}\tilde{h} =& \tilde{M}[\frac{\alpha}{1+\beta'}\mathrm{Cosh}^{-2}(e)\dot{e} - \alpha K_2\chi + \alpha^2\mathrm{Tanh}(e) - \ddot{q}_d] + \frac{\alpha}{1+\beta'}\mathrm{Cosh}^{-2}(e)M_o(q_d)(\dot{e}-\dot{\hat{e}})\\ &+ \tilde{C}[-\dot{q}_d + \frac{\alpha}{1+\beta'}\mathrm{Tanh}(e) + \alpha\chi] - C(q,\dot{q})\dot{\hat{e}} - \tilde{F} - \tilde{G} - M(q)\ddot{\tilde{X}}_1\end{aligned} \tag{27}$$

where M_o, C_o, G_o and F_o are nominal model introduced in (5). $\tilde{M}$, $\tilde{C}$, $\tilde{F}$ and $\tilde{G}$ denote the error between the nominal and true value, and are defined as

$$\tilde{\Sigma} = \Sigma(q,\dot{q}) - \Sigma_o(q_d,\dot{q}_d) = \Sigma(q,\dot{q}) - \Sigma(q_d,\dot{q}_d) - \Delta\Sigma(q_d,\dot{q}_d)$$

for all $\Sigma \in \{M, C, F, G\}$.

Remark 6. Note that, $\hat{h}$ is an available term as it only depends on q_d, $\dot{q}_d$, χ, e, $\dot{\hat{e}}$ and nominal model M_o, C_o, G_o, F_o given in (5). One feature that distinguishes the proposed method from existing ones is that we take full advantage of the prior known information of the plant model and available signals to design the controller. In this way, when compared to the model-free method, the proposed controller can automatically achieve better performance when the nominal model is relatively accurate. Moreover, q_d and $\dot{q}_d$ are defined by users and hence not prone to be augmented with noise.

Remark 7. According to Assumptions 1 and 2, Property 3, the boundedness of $\hat{h}$, $\tilde{h}$ are not difficult to obtain through the analysis of boundedness of each term in (26) and (27).

Finally, we have the dynamics in terms of r as

$$M(q)\dot{r} = -C(q,\dot{q})\dot{r} - \alpha M(q)K_1 r + \hat{h} + \Delta f + \tau \quad \text{with} \quad \Delta f = \tilde{h} - T_d \tag{28}$$

which lumps parametric uncertainties $\tilde{h}$ and external disturbances T_d together.

To compensate the "lumped uncertainties" with a RBF-NN, Δf is parameterized into a form similar to (2) as follows

$$\Delta f = W^\top \sigma(z) + \epsilon(z) \tag{29}$$

where $z = [1, \hat{X}_1, \hat{X}_2, q_d, \dot{q}_d, \ddot{q}_d]^\top \in \mathbb{R}^{5n+1}$, and the definitions of the weight matrix $W \in \mathbb{R}^{\mathcal{L}\times n}$, the activation function $\sigma(z) \in \mathbb{R}^{\mathcal{L}}$ and the small mismatch $\epsilon(z) \in \mathbb{R}^n$ are given in Section 2.

Let the estimate of Δf given by

$$\Delta \hat{f} = \hat{W}^\top \sigma(z) \tag{30}$$

where $\hat{W} \triangleq [\hat{W}_1, \cdots, \hat{W}_n] \in \mathbb{R}^{l\times n}$ denotes the estimate of the ideal weight matrix W. The update law of $\hat{W}$ are

$$\begin{aligned}
\dot{\hat{W}}_i &= \begin{cases} \Gamma \dot{w}_i, & \text{if } g_i < 0 \text{ or } g_i = 0 \text{ with } \dot{\hat{W}}_i^\top \nabla g_i \le 0 \\ \Gamma \dot{w}_i - \Gamma \dfrac{\nabla g_i \nabla g_i^\top}{\nabla g_i^\top \Gamma \nabla g_i} \Gamma \dot{w}_i, & \text{otherwise} \end{cases} \\
\dot{w} &= \sigma(z)\dot{\hat{e}}^\top + \sigma(z)\left(\frac{\alpha}{1+\beta'}\mathrm{Tanh}(e) + \alpha\chi\right)^\top - \rho\hat{W}
\end{aligned} \tag{31}$$

where $\rho, \Gamma \in \mathbb{R}$ are positive constants, $w \triangleq [w_1, \cdots, w_n] \in \mathbb{R}^{l\times n}$, $\dot{\hat{e}} \triangleq \dot{\hat{X}}_1 - \dot{q}_d$, and $g_i(\hat{W}_i) = \hat{W}_i^\top \sigma(z) - \iota_i \tau_N$ for $i \in I_n$. Define $\iota \triangleq [\iota_1, \iota_2, \cdots, \iota_n]^\top$. Note that, the adaptive law (31) leads to a bounded estimate $\Delta\hat{f}$ by employing a standard projection operation. More importantly, the bounds can be adjusted by tuning the parameter $\iota_i \in (0,1)$ which is a constant parameter determining the proportion of control effort that is devoted to dealing with the uncertainties and is described in Section 5.

Remark 8. The number of neurons and the value of p_i, which is the variance of the activation function, are related to the size of approximation error ϵ_N and should be selected carefully. But the optimal design of NN is out of scope of this paper.

Referring to the dynamics (28), the overall control law is proposed as:

$$\tau = K_1 \chi - \hat{h} - \Delta\hat{f} \tag{32}$$

with K_1 being a positive tuning gain matrix and variables χ, $\hat{h}$, $\Delta\hat{f}$ are defined in (21), (26) and (30), respectively.

The requirement of the tuning parameters and the characteristic of the proposed controller subject to Problem 1 described in Section 2 will be rigorously discussed in the following section.

5 | ANALYSIS OF CONVERGENCE OF TRACKING ERROR AND BOUNDEDNESS OF THE CONTROL INPUT

This section is first devoted to the stability analysis of the closed-loop system, and then the boundedness of control input τ is rigorously proved. The main properties of the proposed controller are summarized in the following theorem.

Theorem 2. Suppose Assumptions 1-2 hold, the trajectories of the closed-loop system consisting of (4), (13), (16), (31) and (32) are all bounded and the tracking error will asymptotically converge to the neighborhood of origin IF the control gains α, K_1 and K_2 satisfy the following conditions:

$$\alpha > \frac{5+5\beta'}{4} \tag{33}$$

$$\lambda_{min}(K_1) > \frac{1}{2\alpha \underline{m}} \tag{34}$$

$$\lambda_{min}(K_2) > 0 \tag{35}$$

Furthermore, the norm bound of the tracking error is proportional to the tuning parameters and the "lumped uncertainties". ◁

The Proof of Theorem 2 is presented in Appendix A.2.

Next, we are going to derive the conditions on tuning parameters to ensure the control input τ is bounded and, moreover, bounded by the actuator limits τ_N stated in Problem 1. To this end, a lemma on the boundedness $\xi(t)$ is first presented, which is fundamental to the sequel analysis.

Lemma 1. Suppose Assumption 1 hold, the auxiliary signal $\chi(t)$ governed by (21) satisfies $\|\chi(t)\| \leq 1$ for all $t \geq 0$, if tuning gains α, K_1 and K_2 meet the following condition:

$$\lambda_{min}(K_2) \geq \lambda_{max}(K_1)(B_{ov} + \frac{\alpha}{1+\beta'}) + (1 - \lambda_{min}(K_1))\alpha \tag{36}$$

where B_{ov} denotes the norm bound of the error of estimated velocity $\|\dot{\hat{e}}\|$, whose existence is guaranteed by (7) and the projection operation in (16). ◁

The proof of Lemma 1 can be found in Appendix A.4. Given $\chi(t)$ norm-bounded by 1, the following theorem presents two more conditions on tuning parameters such that one can freely render the upper bounds of the control effort.

Theorem 3. Suppose Assumptions 2 hold and the conditions in Theorem 2 and Lemma 1 are verified. Given $\tau_N \geq \tau_N^* > 0$, if the following inequalities

$$0 < \iota_i \leq 1 - \frac{g_{1i}(\alpha, K_{1i}, K_{2i}) + g_{2i}(B_v, B_a)}{\tau_N} \tag{37}$$

are verified by proper choices of α, K_1, K_2, B_v and B_a, then the control law τ given by (32) is guaranteed to be bounded by the τ_N, that is

$$|\tau_i| \leq \tau_N, \quad \text{for all } i \in I_n$$

where g_{ji}, $j = 1, 2$, are defined in (A21) and (A22), τ_N^* is a known constant given in (A28). ◁

The Proof of Theorem 3 is provided in Appendix A.3.

Remark 9. It can be seen from the right-hand side of (37), in the case of a fixed τ_N, that the greater the term related to the uncertainties of the model (i.e. g_{1i}), the smaller the feasible range of B_v and B_a (i.e. g_{2i}). This is consistent with the intuition in control practice since given a limited control effort τ_N, the trade-off between the performance and robustness of the controlled plant is inevitable. However, for many existing adaptive-based and/or neural network-based techniques, the relation between the control specifications and tuning parameters is implicit. While, for the presented algorithm, one can easily decrease ι to allocate more control efforts to handle the uncertainties rather than to achieve fast and accurate tracking, and vice versa.

Remark 10. For the proposed controller, adjusting control gains α, K_1, and K_2 is necessary to solve Problem 1. Simulations show that a solution exists under reasonable model uncertainties and desired trajectory settings. While trial and error can address the problem, if the conditions (33), (34), (35) and (36), are satisfied, we offer a parameter selection guideline. First, select an appropriate α based on condition (33) for desired error convergence precision. Smaller α leads to better error convergence. However, from condition (34), smaller α results in a larger K_1, potentially causing faster convergence of the tracking error with larger overshoot, as per controller (32). K_2's choice follows similar principles in conditions (35) and (36). This guide helps users adjust control parameters for the desired response.

6 | NUMERICAL EXPERIMENT

We carry out numerical examples on a MATLAB/SIMULINK environment to demonstrate the effectiveness of our controller. A fourth-order Runge-Kutta discretization method with sampling time $T_s = 0.001$s is employed in all simulations.

Consider a two-link robot manipulator system[37] Section III described by :

$$M = \begin{bmatrix} M_{11} & M_{12} \\ M_{12} & M_{22} \end{bmatrix}, C = \begin{bmatrix} C_{11} & C_{12} \\ C_{21} & C_{22} \end{bmatrix}, F = \begin{bmatrix} F_1 \\ F_2 \end{bmatrix}, G = \begin{bmatrix} G_1 \\ G_2 \end{bmatrix}$$

where

$$\begin{aligned} M_{11} &= m_1 l_1^2 + m_2(l_1^2 + l_2^2 + 2l_1 l_2 \cos q_2) + I_1 + I_2, \quad M_{12} = m_2(l_2^2 + l_1 l_2 \cos q_2) + I_2, \quad M_{22} = m_2 l_2^2 + I_2 \\ C_{11} &= -m_2 l_1 l_2 \dot{q}_2 \sin q_2, \quad C_{12} = -m_2 l_1 l_2 (\dot{q}_1 + \dot{q}_2) \sin q_2, \quad C_{21} = m_2 l_1 l_2 \dot{q}_1 \sin q_2, \quad C_{22} = 0, \\ F_1 &= 0.5\dot{q}_1, \quad F_2 = 0.5\dot{q}_2, \quad G_1 = (m_1 l_2 + m_2 l_1) g \cos q_1 + m_2 l_2 g \cos(q_1 + q_2), \quad G_2 = m_2 l_2 g \cos(q_1 + q_2) \end{aligned}$$

with $I_1 = \frac{1}{4}m_1 l_1^2$, $I_2 = \frac{1}{4}m_2 l_2^2$ and the mass, as well as the length parameters, of the manipulator are taken from the datasheet of the Kinova Gen2 manipulator as $m_1 = 1.7$ kg, $m_2 = 2.0$ kg, $l_1 = 0.41$ m, $l_2 = 0.41$ m, $g = 9.8$ m/s^2. The desired trajectory to be tracked is given by:

$$q_d = [\sin(0.5t) \quad \cos(0.5t)]^\top.$$

Parameters of the controller (32) are set to be $K_1 = \text{diag}\{1.8, 1.8\}$, $K_2 = \text{diag}\{49.8, 49.8\}$, $\beta = 1.5$, $\alpha = 11$ and $\iota = [0.5, 0.5]^\top$, while the parameters of RBF NN (30) are $\Gamma = 30I$, $p_{ik} = 1.5$, μ_i evenly located in $[-3, 3]$, $\rho = 0.001$. For the observer (16), we choose $\theta = 0.7$ and $l = 130$. The lower and upper actuation saturation limits are given as -40 and 40 Nm, i.e., $\tau_N = 40$.

Additional initialization values used in the sequel simulations are: $q(0) = [0.5, 0.5]^\top$ rad, $\dot{q}(0) = [0, 0]^\top$ rad/s, $\hat{W}(0) = \mathbf{0}_{30\times 2}$, $\hat{X}_1 = [0, 0]^\top$ rad, $\hat{X}_2 = [0, 0]^\top$ rad/s and $\hat{X}_3 = [0, 0]^\top$.

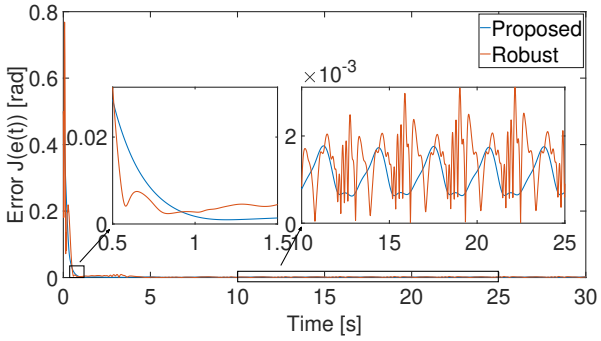

FIGURE 2 Trajectory tracking error in the nominal case.

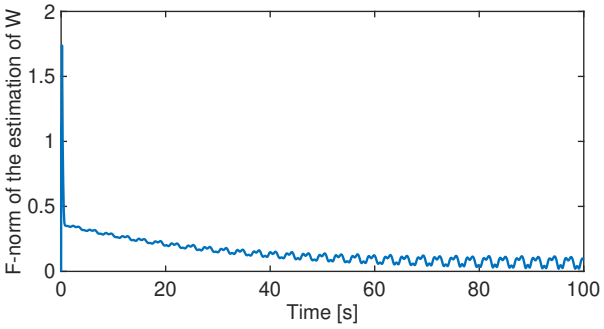

FIGURE 3 Time evolution of $\|\hat{W}\|_F$ in the nominal case.

We compare our method against a state-of-the-art robust adaptive control scheme[38]. For the sake of comparison fairness, we first tune both methods to achieve a comparable behavior (similar convergence speed with similar steady-state error) in the absence of the input constraints, model uncertainties and disturbances.

As shown in Fig.2, let both methods track q_d with sufficiently small error after around 0.5s, we obtain the gain parameters of the robust adaptive controller[38] are: $K_p = 10.6$, $K_d = 15.1$, $K_r = 0002$, $K_\beta = 10$, $\Gamma_q = 16.5$, $\Gamma_z = 12.5$. The performance criteria show there is the root mean square error (RMSE) of tracking trajectories, defined as $J(e(t)) = \sqrt{\frac{1}{2}(e_1^2 + e_2^2)}$, in which $e_i, i = 1, 2$, denote the tracking error of joint i. The input torque is illustrated in Fig. 4. Note that a robust controller has a large overshoot during the transient period while the proposed method features a smooth maneuver that is kept in a small range, which validates the effectiveness of the proposed controller. The convergence of the $\|\hat{W}\|_F$ is illustrated in Fig. 3, where, to better illustrate the convergence behavior of the neural network, we have extended the runtime to 100 seconds.

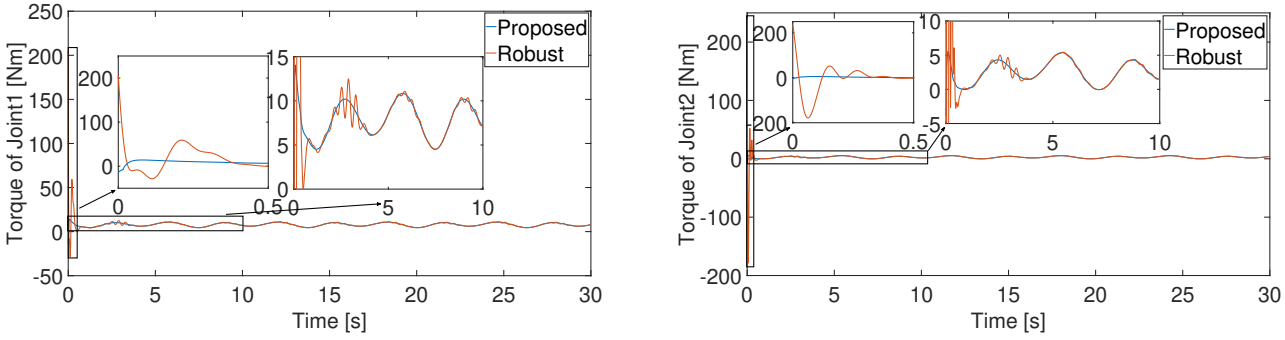

FIGURE 4 Time evolution of the input torque of joints without actuator limitations.

In the following simulation, we assess the influence of model uncertainties, external disturbances and input constraints on the two algorithms, and therefore, show the strength of the proposed scheme. The choices of tuning parameters are kept the same as the ideal case. Furthermore, a large model mismatch $\mu_{unc} = 50\%$ is selected in the following way to show the robustness of the proposed algorithm:

$$m_1' = (1 + \mu_{unc})m_1, \quad m_2' = (1 + \mu_{unc})m_2, \quad l_1 = (1 + \mu_{unc})l_1, \quad l_2 = (1 + \mu_{unc})l_2$$

where m_1', m_2', l_1', l_2' are the actual parameters considered in the manipulator system. Gaussian Noise with a mean of 5 rad and variance of 5 rad^2 is added to the input signal, starting from 15s. The limit of torque of actuators output is taken as $\tau_N = 40$ Nm.

From Fig.5, one can immediately observe that the robust controller is no longer a stabilizing one. As a matter of fact, the degradation of tracking performance or even instability due to the non-linearity introduced by the saturated operation on the control signals are rather common phenomena in control. In this connection, our controller is completely free of this issue by accounting for the limitations of the actuators at the beginning of the control law design. As shown in Fig.7, the proposed controller indeed never exceeds the limitation of the actuator, while the robust method suffers from a fast switching between the positive and negative boundaries. Apart from the loss of stability, the switching-like behavior of the torque may also damage the actuators and waste energy. This implies the superiority of the proposed scheme. Naturally, if we further decrease the upper bounds of the actuators τ_N, tuning parameters like α, K_1 and K_2 need to be re-selected, and the tracking ability of the controller will be influenced as well. But as long as we have prior knowledge of the lower bounds of the actuator limits, the ISS with respect to the lumped uncertainties and boundedness of the overall trajectories are always ensured by the proposed scheme. Unlike in Fig. 3, the $\|\hat{W}\|_F$ in Fig. 6 is unable to converge to a constant value, primarily due to the impact of model uncertainty and external disturbances.

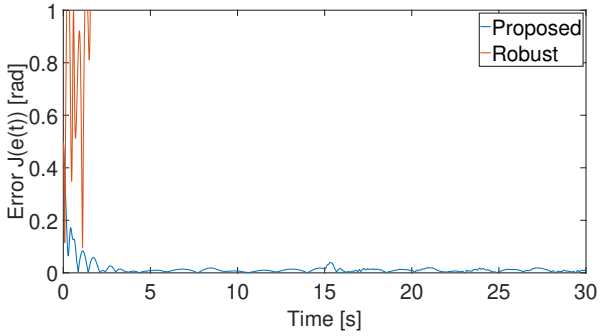

FIGURE 5 Trajectory tracking error in non-ideal case.

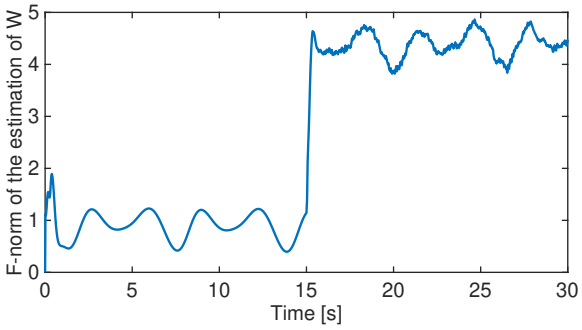

FIGURE 6 Time evolution of $\|\hat{W}\|_F$ in non-ideal case.

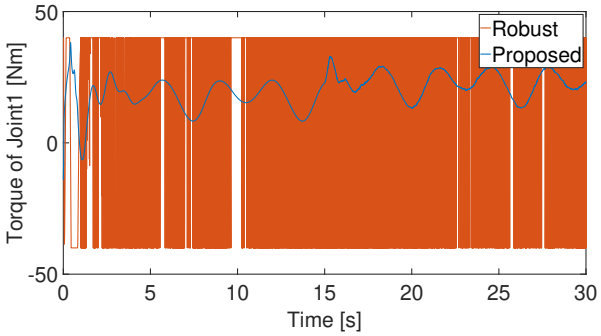

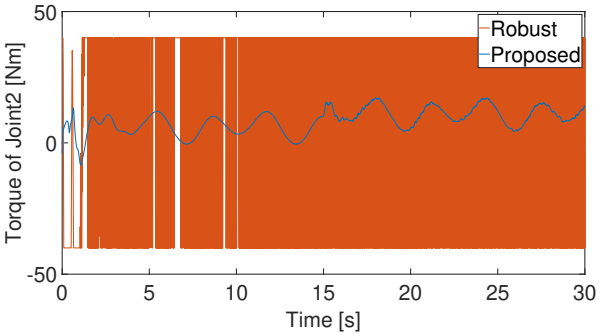

FIGURE 7 Time evolution of the input torque of joints in non-ideal case.

7 | EXPERIMENT ON KINOVA GEN2 ROBOT

In this section, a real-world experiment is performed on a 6-DOF Kinova Gen2 robot arm (Kinova Inc., Canada) and shown in Fig. 8, to further assess the performance of the proposed controller. The control algorithm is programmed in Python and C++, and executed by a computer using the Ubuntu 18.04 Linux operating system, where the computer has 16.0 GB RAM and an Intel Core i5-7300HQ CPU with 1.6 GHz. The computer communicates with the Kinova Gen2 robot through ROS Melodic Morenia. For simplicity, only the second and third joints from shoulder to end-effector are used to test the proposed method. A classical Kalman filtering algorithm[39] is employed to address the noise signals present in the data collected by sensors. The desired trajectories of joints are chosen as:

$$q_d(t) = [\sin(0.5t) + 1.5 \quad \sin(0.5t)]^\top$$

which is feasible in the sense that perfect trajectory tracking does not require control efforts that exceed the actuator limits $\tau_N \geq 10$ Nm.

FIGURE 8 The Kinova Gen2 robot.

The parameter settings and initial conditions that are different from the previous numerical examples are $K_1 = \text{diag}\{2, 2\}$, $K_2 = \text{diag}\{6, 6\}$, $\beta = 9$, $\alpha = 3, l = 200$, $q(0) = [1.5, 0]^\top$ rad and $\hat{X}_1 = [1.5, 0]^\top$ rad. The inconsistency of the tuning parameters is partial because of the different settings of the sampling time where in the real experiment, $T_s = 0.01$s, while that of the simulation experiment is 0.001s. To demonstrate the advantages of the proposed method, we apply a PID algorithm to the Kinova robot whose values of the parameter are $P = 3.5$, $I = 0.5$ and $D = 4.1$.

The results shown in Fig. 9-13 depict the test results of the proposed algorithm and the classical PID algorithm on two joints of the Kinova Gen2 robot. From Fig. 9 and Fig. 10, it can be observed that both algorithms can track the reference trajectories with bounded tracking errors. However, our proposed algorithm exhibits smaller trajectory tracking errors and smaller overshoots. In Fig. 11 and Fig. 12, it is evident that the torque signals generated by our proposed algorithm are smoother and remain within a relatively small range without violating the predetermined input constraints. Fig. 13 illustrates the velocity tracking errors of our proposed algorithm. However, tracking errors are higher in the real world when compared to simulation results. This is mainly due to the fact that the position measurements provided by the embedded sensors do not accurately present the true angular position of each joint, which leads to a significant observer error in the velocity information. This observation also motivates the further improvement of the robustness of the scheme with respect to the sensor noise.

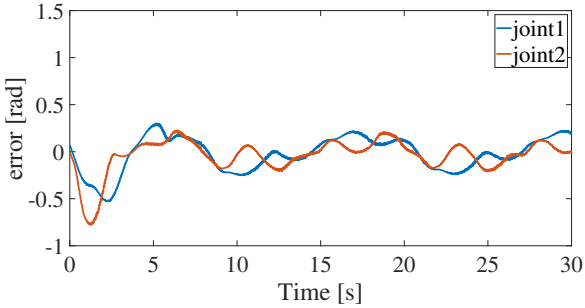

FIGURE 9 Trajectory tracking error of the proposed controller.

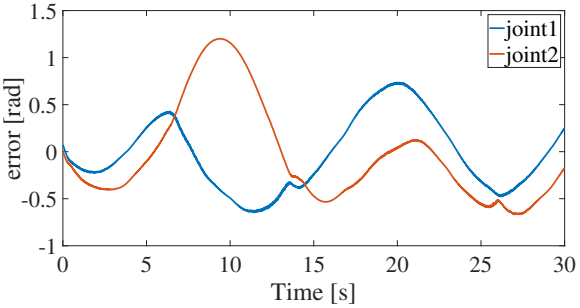

FIGURE 10 Trajectory tracking error of PID.

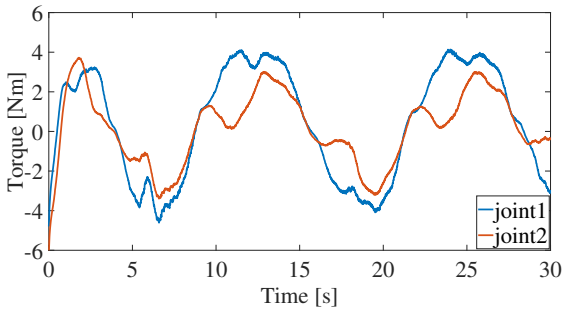

FIGURE 11 Input torque of the proposed controller.

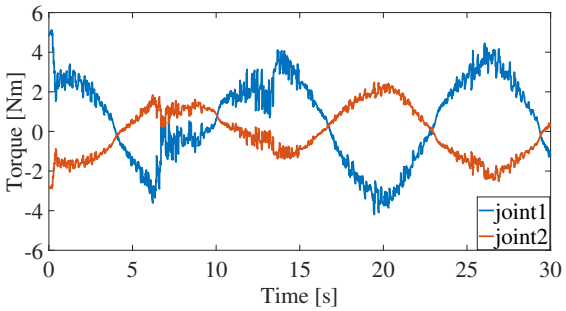

FIGURE 12 Input torque of PID.

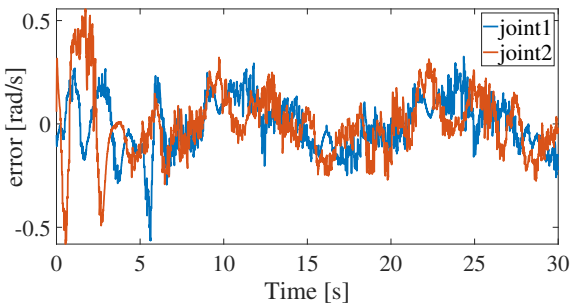

FIGURE 13 Time evolution of the velocity error of the proposed controller.

8 | CONCLUDING REMARKS

In this paper, given only the angular position measurements, the trajectory tracking problem for a manipulator system under the influence of the model uncertainties, external disturbances and input constraints is addressed. The problem is quite involved in the sense that the system is highly nonlinear and strong robustness of a limited control input is requested. Our solution to this problem is composed of a novel NN-based adaptive controller and a modified ESO. The first novelty of the proposed scheme lies in the fact that we achieve an adjustable bounded control law by utilizing projection operations and an auxiliary term admitting the $\tanh(\cdot)$ form to avoid using a saturation function which in general will degrade the performance of the original controller. Secondly, in terms of uncertainties, if a sufficiently accurate nominal model is indeed available and the external disturbances are negligible, the controller can be transformed into a completely model-based one by simply setting the parameter $\iota = 0$. Meanwhile, the structure and other features (stabilizing and boundedness) of the controller are entirely preserved. Similarly, the gain tuning for large lumped uncertainties scenarios can also be easily done by selecting ι. This feature significantly enhances

the generality of the proposed controller and might be favorable to the practitioners, as no control law or adaptive law redesign is needed. The effectiveness of the proposed scheme is verified in both simulation and real-world environments, where we notice the sensitivity of the presented controller with respect to large measurement noise. This motivates the first future work direction. Another one currently under investigation is to consider the state and/or output constraints.

9 | ACKNOWLEDGEMENT

This work was supported in part by the Yangfan Program of Shanghai, China, under Grant 21YF142960. The authors thank Dr. Andre Rosendo for his very helpful comments on earlier drafts of this paper.

□

APPENDIX

A PROOF SUPPORTS

A.1 Proof of Theorem 1

The proof is done in two steps. First, consider the observer (13) without the project operation (16) and prove the properties claimed in the theorem hold. Then, we show that the projection operator will not spoil the obtained features.

To make the paper self-contained, we introduce the Tube lemma that is essential to the following proof.

Lemma 2. (Tube lemma[40]): Consider the product space $X \times Y$ where Y is compact. If N is an open set of $X \times Y$ containing the slice $\{x_0\} \times Y$ of $X \times Y$, then N contains some tube $W \times Y$ about $\{x_0\} \times Y$, where W is a neighborhood of x_0 in X. ◁

Let

$$\eta_i(t) = \begin{bmatrix} \eta_{i1}(t) \\ \eta_{i2}(t) \\ \eta_{i3}(t) \end{bmatrix} = L \begin{bmatrix} x_{i1}(t) - \hat{x}_{i1}(t) \\ x_{i2}(t) - \hat{x}_{i2}(t) \\ x_{i3}(t) - \hat{x}_{i3}(t) \end{bmatrix}, \quad i \in I_n \tag{A1}$$

represent the re-scaled observer error with L being

$$L \triangleq \text{diag}\{l^2, l, B_f\} \in \mathbb{R}^{3\times 3} \tag{A2}$$

In view of (11) and (13), we can write the dynamic equation of $\eta_i(t)$ as

$$\dot{\eta}_i = lg(\eta_i) + \Phi_i, \quad g(\eta_i) = \begin{bmatrix} \eta_{i2} - k_{i1} g_1(\eta_{i1}) \\ \eta_{i3} - k_{i2} g_2(\eta_{i1}) \\ -B_f k_{i3} g_3(\eta_{i1}) \end{bmatrix}, \quad \Phi_i(t) = \begin{bmatrix} 0 \\ 0 \\ B_f \dot{x}_{i3}(t) \end{bmatrix} \tag{A3}$$

Obviously, given Assumption 2 holds, there exist a constant $\zeta_{\Phi_i} > 0$ such that $\|\Phi_i(t)\| \leq \zeta_{\Phi_i}$. In addition, if θ in (14) equals to 1, (A3) can be further written as

$$\dot{\eta}_i = lK_i\eta_i + \Phi_i \tag{A4}$$

Consider a Lyapunov function as follows:

$$V(\theta, \eta) = \sum_{i=1}^{n} V_i(\theta, \eta_i), \quad V_i(\theta, \eta_i) = \eta_i^\top P_i \eta_i \tag{A5}$$

in which P_i is a symmetric positive definite matrix solution to the Lyapunov equation $K_i^\top P_i + P_i K_i = -I$ with I being an identity matrix. Considering $\theta = 1$, the time derivative of $V_i(\theta, \eta_i)$ along the solution of (A4) can be obtained as follows:

$$\frac{dV_i(1, \eta_i)}{dt} = -l\|\eta_i\|^2 + 2\eta_i^\top P_i \Phi_i \leq -\frac{l}{2}\|\eta_i\|^2 + \frac{\zeta_{\Phi_i}^2}{l}(\lambda_{max}(P_i))^2 \tag{A6}$$

which implies that, for all $l > 0$, system (A3) is ISS and there exist $\mathcal{KL}$ functions to meet (18) when $\theta = 1$.

Furthermore, as V_i is proper[2], for all $i \in I_n$, $R_i = \{\eta_i \in \mathbb{R}^3 : V_i(1,\eta_i) = \varkappa_i\}$ is a compact set of $\mathbb{R}^3$ [40], with $\varkappa_i \in [\inf_{t\geq 0} V_i(1,\eta_i), \sup_{t\geq 0} V_i(1,\eta_i)]$. Let the function $\varphi_i : \mathbb{R}_{>0} \times R_i \to \mathbb{R}$ be the map of $(\theta,\eta_i) \mapsto \langle \nabla V_i(\theta,\eta_i), \dot{\eta}_i\rangle$, in which $\dot{\eta}_i$ is defined in (A3). Since φ_i^{-1} is an open subset of $\mathbb{R}_{>0} \times R_i$ containing the slice $\{1\} \times R_i$ and R_i is compact, it follows from the Lemma 2 that φ_i^{-1} contains some tube $(1-\epsilon_i, 1+\epsilon_i) \times R_i$ about $\{1\} \times R_i$, where $\epsilon_i \in (0,1)$. Then, for all $l > 0$ and $(\theta,\eta_i) \in (1-\epsilon_\theta, 1+\epsilon_\theta) \times R_i$, we can draw a conclusion that the system (A3) is ISS by defining $\epsilon_\theta \triangleq \cap_{i\in I_N} \epsilon_i$ to meet all n subsystems, and there exist $\mathcal{NL}$ functions to meet (18). This completes the first part of the proof of the Theorem 1.

Next, let's include the projection (16) into the velocity observer, and the dynamic of re-scaled observer error η_i becomes

$$\dot{\eta}_i = lg(\eta_i) + \Phi_i + Q_i, \quad \text{with} \quad Q_i = \begin{cases} \frac{P_i^{-1}L^{-1}\hat{x}_i\hat{x}_i^\top\Lambda^\top\Lambda}{\hat{x}_i^\top\Lambda^\top\Lambda\Lambda^\top\Lambda\hat{x}_i}\dot{\hat{x}}_i, & \|\Lambda\hat{x}_i\| = S_i \text{ and} \dot{\hat{x}}_i^\top\Lambda^\top\Lambda\hat{x}_i > 0 \\ \mathbf{0}, & \text{otherwise} \end{cases} \tag{A7}$$

where $\Lambda^\top\Lambda \triangleq L^{-1}P_i^{-1}L^{-1}$ with L and P_i are symmetric positive definite matrix defined in (A2) and (A5), respectively[3]. It's straightforward to see that, when $Q_i \neq \mathbf{0}$, the time derivative of $V_i(\theta,\eta_i)$ will have an addition term $\eta_i^\top P_i Q_i$ given by

$$\eta_i^\top P_i Q_i = \begin{bmatrix} x_{i1}-\hat{x}_{i1} \\ x_{i2}-\hat{x}_{i2} \\ x_{i3}-\hat{x}_{i3} \end{bmatrix}^\top \begin{bmatrix} \hat{x}_{i1} \\ \hat{x}_{i2} \\ \hat{x}_{i3} \end{bmatrix} \frac{\hat{x}_i^\top\Lambda^\top\Lambda}{\hat{x}_i^\top\Lambda^\top\Lambda\Lambda^\top\Lambda\hat{x}_i}\dot{\hat{x}}_i \tag{A8}$$

Thanks to the convexity of hyper-sphere S_i, we have $(x_{ij}-\hat{x}_{ij})^\top\hat{x}_{ij} \leq 0$, for $j \in \{1,2,3\}$, when $\|\Lambda\hat{x}_i\| = S_i$. Together with $\dot{\hat{x}}_i^\top\Lambda^\top\Lambda\hat{x}_i = \hat{x}_i^\top\Lambda^\top\Lambda\dot{\hat{x}}_i > 0$, it follows that $\eta_i^\top P_i Q_i \leq 0$. One can see that, the addition term introduced by the projection can only make the derivative of $V_i(\theta,\eta_i)$ more negative and therefore does not affect the previous results. This completes the proof.

A.2 Proof of Theorem 2

Defining $\varsigma = [e^\top, r^\top, \chi^\top, \sqrt{Q}]^\top \in \mathbb{R}^{3n+1}$ with $Q := \frac{1}{2}tr(\tilde{W}^\top\Gamma^{-1}\tilde{W})$, we are going to prove the boundedness of trajectories of the closed-loop system via the boundedness of ς. First, substitute the control law (32) into (28) to obtain the dynamic equation in terms of r as follows:

$$M(q)\dot{r} = -C(q,\dot{q})r - \alpha M(q)K_1 r + K_1\chi + \tilde{W}^\top\sigma(z) + \epsilon(z) \tag{A9}$$

with $\tilde{W}(t) \triangleq W - \hat{W}(t) \in \mathbb{R}^{\mathcal{L}\times n}$ denoting the estimation error between the ideal weight matrix and the actual weight matrix. Consider the following candidate Lyapunov function:

$$V(\varsigma) = \sum_{i=1}^{n} \ln[\cosh(e_i)] + \frac{1}{2}r^\top Mr + \frac{1}{2}\chi^\top\chi + Q$$

Thanks to the fact that $\ln[\cosh(||x||)] \leq ||x||^2$ for any column vector x, it is easy to bound $V(\varsigma)$ from below and above as follows

$$\rho_1 \ln(\cosh(||\varsigma||)) \leq V \leq \rho_2||\varsigma||^2 \tag{A10}$$

with some positive constants $\rho_1 \triangleq \min\frac{1}{2}\{1, \underline{m}\}$, $\rho_2 \triangleq \max\{1, \frac{1}{2}\overline{m}\}$.

In view of (20), (21) and (A9) and the relation $\dot{e} = \dot{\hat{e}} + \dot{\tilde{X}}_1 = \dot{\hat{e}} + \tilde{X}_2$ with $\dot{\tilde{X}}_1$, $\tilde{X}_2$ are defined in (19), we have the time derivative of $V(\varsigma)$ along the solution of closed-loop system is given by

$$\begin{aligned}
\dot{V} =& -\frac{\alpha}{1+\beta'}\text{Tanh}^\top(e)\text{Tanh}(e) + \text{Tanh}^\top(e)r - \alpha\text{Tanh}^\top\chi(e) + \text{Tanh}^\top(e)\tilde{X}_2 + \frac{1}{2}r^\top\dot{M}r + \frac{1}{2}r^\top[-2C(q,\dot{q})r] \\
&+ r^\top[-\alpha M(q)K_1 r + K_1\chi + \tilde{W}^\top\sigma(z) + \epsilon(z)] + \chi^\top[-K_1 r - K_2\chi + \alpha\text{Tanh}(e)] - tr(\tilde{W}^\top\Gamma^{-1}\dot{\hat{W}}) \\
=& -\frac{\alpha}{1+\beta'}\text{Tanh}^\top(e)\text{Tanh}(e) + \text{Tanh}^\top(e)\tilde{X}_2 - \chi^\top K_2\chi - \alpha r^\top M(q)K_1 r + \text{Tanh}^\top(e)r + r^\top\epsilon(z) + r^\top\tilde{W}^\top\sigma(z) - tr(\tilde{W}^\top\Gamma^{-1}\dot{\hat{W}}) \\
\leq& -\frac{\alpha}{1+\beta'}||\text{Tanh}(e)||^2 + \|\text{Tanh(e)}\|\|\tilde{X}_2\| - \lambda_{min}(K_2)\|\chi\|^2 - \alpha\underline{m}\lambda_{min}(K_1)\|r\|^2 + \|\text{Tanh}(e)\|\|r\| + ||r||\|\epsilon(z)\| \\
&+ r^\top\tilde{W}^\top\sigma(z) - tr(\tilde{W}^\top\Gamma^{-1}\dot{\hat{W}})
\end{aligned} \tag{A11}$$

[2] Proper map, in topology, a property of continuous function between topological spaces, if inverse images of compact subsets are compact

[3] A symmetric positive definite matrix can be represented as the product of a lower triangular matrix, which have all positive eigenvalues, and its transpose, also known as Cholesky decomposition.

where the vector function $\text{Tanh}(e) \triangleq [\tanh(e_1), \cdots, \tanh(e_n)]^\top$ and we have taken advantage of the relation that

$$\frac{d}{dt}\sum_{i=1}^{n}\ln[\cosh(e_i)] = \sum_{i=1}^{n}\tanh(e_i)\dot{e}_i = \text{Tanh}^\top(e)\dot{e}.$$

Thanks to (20), (31) and the fact that $\tanh(x) \leq x$ for $x \geq 0$, $tr(xy^\top) = x^\top y$ for all column vector $x, y \in \mathbb{R}^n$, we can further derive the upper bound of the last two-term of $\dot{V}$ as

$$\begin{aligned} &r^\top\tilde{W}^\top\sigma(z) - tr(\tilde{W}^\top\Gamma^{-1}\dot{\hat{W}}) = r^\top\tilde{W}^\top\sigma(z) - tr\left(\tilde{W}^\top\sigma(z)(\dot{\hat{e}}^\top + \frac{\alpha}{1+\beta'}\text{Tanh}^\top(e) + \alpha\chi^\top) - \tilde{W}^\top\rho\hat{W}\right) \\ &= [\tilde{W}^\top\sigma(z)]^\top r - tr\left(\tilde{W}^\top\sigma(z)r^\top\right) - tr\left(\rho\tilde{W}^\top\hat{W}\right) = tr(\rho\tilde{W}^\top\hat{W}) = tr(\rho\tilde{W}^\top(W-\tilde{W})) \leq -\frac{\rho}{2}\|\tilde{W}\|_F^2 + \frac{\rho}{2}\|W\|_F^2 \end{aligned} \tag{A12}$$

where we have neglected the effect of projection operation, as it only makes the time derivative more negative. The rigorous derivation in the case that there exists projection of NN follows the proof of Lemma 4 of in[41] Chapter 3.

Next, utilizing Property 2, Property 3 and (A12), we have

$$\dot{V} \leq -\frac{\alpha}{1+\beta'}||\text{Tanh}(e)||^2 + \|\text{Tanh(e)}\|\|\tilde{X}_2\| + \|\text{Tanh}(e)\|\|r\| - \alpha\underline{m}\lambda_{min}(K_1)||r||^2 + \epsilon_N||r|| - \lambda_{min}(K_2)||\chi||^2 - \frac{\rho}{2}\|\tilde{W}\|_F^2 + \frac{\rho}{2}W_B$$

where W_B is a positive constant whose value is proportional to the lumped uncertainties. Finally, applying Young's inequalities to the cross terms in the above inequality, it holds that

$$\|\text{Tanh(e)}\|\|\tilde{X}_2\| \leq \frac{1}{4}\|\text{Tanh}(e)\|^2 + \|\tilde{X}_2\|^2, \quad \|\text{Tanh}(e)\|\|r\| \leq \|\text{Tanh}(e)\|^2 + \frac{1}{4}\|r\|^2, \quad \epsilon_N\|r\| \leq \frac{1}{4}\|r\|^2 + \epsilon_N^2$$

which yields

$$\dot{V} \leq -\left(\frac{\alpha}{1+\beta'} - \frac{5}{4}\right)||\text{Tanh}(e)||^2 - \lambda_{min}(K_2)||\chi||^2 - \left(\alpha\underline{m}\lambda_{min}(K_1) - \frac{1}{2}\right)||r||^2 - \frac{\rho}{2}||\tilde{W}||_F^2 + \|\tilde{X}_2\|^2 + \epsilon_N^2 + \frac{\rho}{2}W_B$$

Bearing in mind the fact that $\tanh^2(||x||) \leq ||\text{Tanh}(x)||^2$ for any column vector $x \in \mathbb{R}^n$, $\dot{V}(t)$ can be further bounded by

$$\dot{V} \leq -\beta_2\tanh^2(||\varsigma||) + \beta_1 \tag{A13}$$

where $\beta_1 = \bar{\kappa}^2 + \epsilon_N^2 + \frac{\rho}{2}W_B$ with $\bar{\kappa} \triangleq [\bar{\kappa_1}, \bar{\kappa_2}, \cdots, \bar{\kappa_n}]^\top$. $\bar{\kappa_i}$, defined in (18), are the upper bound of the estimation errors $\|\tilde{X}_2\|$. $\varsigma = [e^\top, r^\top, \chi^\top, \sqrt{Q}]^\top \in \mathbb{R}^{3n+1}$ with $Q := \frac{1}{2}tr(\tilde{W}^\top\Gamma^{-1}\tilde{W})$ is defined at the beginning of the proof. $\beta_2 \in \mathbb{R}$ is given by

$$\beta_2 = \min\{\frac{\alpha}{1+\beta'} - \frac{5}{4}, \alpha\underline{m}\lambda_{min}(K_1) - \frac{1}{2}, \lambda_{min}(K_2), \frac{\rho}{\lambda_{max}(\Gamma^{-1})}\}. \tag{A14}$$

The positiveness of β_2 is guaranteed by conditions (33)−(35) and β_2 is a term proportional to the size of model uncertainties and external disturbances, thus the closed-loop system is ISS with respect to the "lumped uncertainties". Given this, it is trivial to see that ς is bounded asymptotically enters a small hyper-sphere of the origin whose size depends on tuning parameters and the "lumped uncertainties", which indicates the same boundedness and convergence property of all elements in ς, i.e. e, r, χ and $\tilde{W}$. Now, the only thing left is to show similar property also holds for $\dot{e}$.

Referring to (20), we have $\lim_{t\to\infty}\|\dot{\hat{e}}\| \leq \lim_{t\to\infty}\|r\| + \frac{\alpha}{1+\beta'}\|e\| + \alpha\|\chi\|$ converges to a sufficiently small value as well. Furthermore, thanks to the convergence property stated in Theorem 1 and the relation $\dot{e} = \dot{\hat{e}} + \dot{\tilde{X}}_1$, one can easily conclude that $\dot{e}$ also converges to a small neighborhood of the origin whose size depends on tuning parameters and the "lumped uncertainties". Thus ending the proof.

A.3 Proof of Theorem 3

Rewrite the control law in (32) as

$$\tau_i = K_{1i}\chi_i - \hat{h}_i - \Delta\hat{f}_i, \quad i = 1, 2\cdots n \tag{A15}$$

where χ_i, $\Delta\hat{f}_i$ and $\hat{h}_i$ are i-th row elements of $\Delta\hat{f}$, χ and $\hat{h}$, respectively, and K_{1i} represents its i-th diagonal elements. Thanks to the projection operator (31) in (30), the following inequality holds naturally

$$|\Delta\hat{f}_i| \leq \iota_i\tau_N. \tag{A16}$$

Secondly, benefiting from Lemma 1, one have

$$|K_{1i}\chi_i| \leq |K_{1i}| \tag{A17}$$

For $\hat{h}_i$, which is the i-th element of $\hat{h}$ defined in (26), according to Property 3 and Assumption 1, 2, it holds that

$$|\hat{h}_i| \leq \overline{m}[\frac{\alpha}{1+\beta'}\|\dot{\hat{e}}\| + \alpha\|K_2\| + \alpha^2 + \|B_a\|] + \zeta_c\|B_v\|[\|B_v\| + \frac{\alpha}{1+\beta'} + \alpha] + \zeta_{f_d}\|B_v\| + \zeta_{f_s} + \zeta_g, \quad i \in I_n \tag{A18}$$

Applying Young's inequality to the term $\zeta_c\|B_v\|(\frac{\alpha}{1+\beta'} + \alpha)$ in (A18), we have

$$\zeta_c\|B_v\|(\frac{\alpha}{1+\beta'} + \alpha) \leq \frac{\zeta_c^2\|B_v\|^2}{4\overline{m}} + \overline{m}(\frac{\alpha}{1+\beta'} + \alpha)^2. \tag{A19}$$

In view of (A16)-(A19), together with the bounds of the observation error derived in (A29) of Appendix A.4, we can further bound τ_i by following inequality:

$$\begin{aligned}|\tau_i| \leq & |K_{1i}| + \overline{m}[\frac{\alpha}{1+\beta'}S + \alpha\|K_2\| + \alpha^2 + (\frac{\alpha}{1+\beta'} + \alpha)^2] + \overline{m}\|B_a\| + (\zeta_c + \frac{\zeta_c^2}{4\overline{m}})\|B_v\|^2 + (\overline{m}\frac{\alpha}{1+\beta'} + \zeta_{f_d})\|B_v\| + \zeta_{f_s} + \zeta_g + \iota_i\tau_N \\ = & g_{1i} + g_{2i} + \iota_i\tau_N,\end{aligned} \tag{A20}$$

where K_{1i} represents its i-th diagonal elements, g_{1i} and g_{2i} are defined as follows

$$g_{1i} \triangleq |K_{1i}| + \overline{m}[\frac{\alpha}{1+\beta'}S + \alpha\|K_2\| + \alpha^2 + (\frac{\alpha}{1+\beta'} + \alpha)^2], \tag{A21}$$

$$g_{2i} \triangleq \overline{m}\|B_a\| + (\zeta_c + \frac{\zeta_c^2}{4\overline{m}})\|B_v\|^2 + (\overline{m}\frac{\alpha}{1+\beta'} + \zeta_{f_d})\|B_v\| + \zeta_{f_s} + \zeta_g. \tag{A22}$$

Here, the upper bound of $|\tau_i|$ is divided into three parts, g_{1i} mainly depends on the tuning parameters K_1, K_2 and α while the size of g_{2i} is determined by the parameters relevant to the desired trajectories, i.e. B_a and B_v. In view of (A20) and if ι_i verifies the (37), it can be easily seen that the control law is norm-bounded by

$$|\tau_i| \leq \tau_N, \tag{A23}$$

for all $i \in I_N$, which typifies the boundedness property of the control effort claimed in this theorem. Now, one thing left is to show that the feasible range of tuning parameter ι_i is non-empty. In other words, solutions of inequalities (33)-(37) exist.

To this end, we need to first find the minimum value of g_{1i} given sufficiently small tuning parameters that guarantees the stability of overall system. For any K_1 and K_2 verifying the condition (34)-(36), it holds that

$$\begin{aligned}g_{1i} \geq & \lambda_{min}(K_1) + \overline{m}[\frac{\alpha}{1+\beta'}S + \alpha\lambda_{min}(K_2) + \alpha^2 + (\frac{\alpha}{1+\beta'} + \alpha)^2] \\ \geq & \lambda_{min}(K_1) + \overline{m}[\frac{\alpha}{1+\beta'}S + \alpha \cdot \max\{0, \lambda_{max}(K_1)(B_{ov} + \frac{\alpha}{1+\beta'}) + \alpha - \lambda_{min}(K_1)\alpha\} + \alpha^2 + (\frac{\alpha}{1+\beta'} + \alpha)^2] \\ \geq & \lambda_{min}(K_1) + \overline{m}[\frac{\alpha}{1+\beta'}S + \alpha^2 + (\frac{\alpha}{1+\beta'} + \alpha)^2] \geq \frac{1}{2\alpha\underline{m}} + \overline{m}[\frac{\alpha}{1+\beta'}S + \alpha^2 + (\frac{\alpha}{1+\beta'} + \alpha)^2]\end{aligned} \tag{A24}$$

where B_{ov} represents the upperbound of the estimated velocity's error defined in (A29), $S = \sqrt{S_1^2 + \cdots + S_n^2}$ for $i \in I_n$, and a reasonable value of S_i is defined in (17). Referring to (33), one can see g_{1i} approaches its minimum value as

$$\alpha \to (\frac{5+5\beta'}{4})^+ \tag{A25}$$

where $(\cdot)^+$ represents the right limit at this point, and the proof is placed in Appendix A.5. Hence, one have

$$\inf_{K1,K2,\alpha} g_{1i} = \frac{2}{5(1+\beta')\underline{m}} + \overline{m}[\frac{125}{16} + \frac{75}{8}\beta' + \frac{25}{8}\beta'^2 + \frac{5}{4}S] := \underline{g_{1i}} \tag{A26}$$

As for g_{2i}, consider the extreme case where the desired trajectories are zero signals, we have

$$\inf_{B_v,B_a} g_{2i} = \zeta_{f_s} + \zeta_g := \underline{g_{2i}} \tag{A27}$$

In summary, there exists a non-empty set of tuning parameter and desired trajectories such that,

$$\Delta g := g_{1i} + g_{2i} - \underline{g_{1i}} - \underline{g_{2i}}$$

can be rendered arbitrarily small.

Define

$$\tau_N^* > \frac{2}{5(1+\beta')\underline{m}} + \overline{m}[\frac{125}{16} + \frac{25}{4}\beta' + \frac{25}{8}\beta'^2 + \frac{5}{4}S] + \zeta_{f_s} + \zeta_g \tag{A28}$$

Under the condition that $\tau_N \geq \tau_N^*$, one can see that

$$\underline{g_{1i}} + \underline{g_{2i}} = g_{1i} + g_{2i} - \Delta g < \tau_N.$$

Put it in another way, there always exist α, K_1, K_2, B_v and B_a such that the following inequality is ensured:

$$g_{1i} + g_{2i} < \tau_N$$

Therefore, one can conclude that $1 - \frac{g_{1i}+g_{2i}}{\tau_N} > 0$, i.e., ι_i admits a feasible range to verify condition (37) and in turn ensure the τ_i to be bounded by τ_N. Thus ending the proof.

A.4 Proof of boundedness of $\chi(t)$

Substituting (20) into (21), we have

$$\dot{\chi} = -K_1(\dot{\hat{e}} + \frac{\alpha}{1+\beta'}\text{Tanh}(e) + \alpha\chi) - K_2\chi + \alpha\text{Tanh}(e) = -(K_1\alpha + K_2)\chi + \bar{u}(t), \qquad \chi(0) = 0$$

where $\bar{u}(t) = -K_1(\dot{\hat{e}} + \frac{\alpha}{1+\beta'}\text{Tanh}(e)) + \alpha\text{Tanh}(e)$. In view of (16) and (20), we can bound $\|\dot{\hat{e}}\|$ by

$$\|\dot{\hat{e}}\| \leq \|\dot{\hat{q}}\| + \|\dot{q}_d\| \leq S + \|B_v\| \triangleq B_{ov} \tag{A29}$$

where B_v is defined in (7), $S = \sqrt{S_1^2 + \cdots + S_n^2}$ with S_i given by, for instance, (17).

Since α, K_1 and $\text{Tanh}(\cdot)$ all feature an upper bound, the norm-bounded of $\bar{u}(t)$, can be easily derived as

$$\|\bar{u}(t)\| \leq \zeta_{\bar{u}} := \lambda_{\max}(K_1)(B_{ov} + \frac{\alpha}{1+\beta'}) + \alpha$$

which yields

$$\chi \leq \int_0^t e^{-(K_1\alpha+K_2)(t-\tau)}\zeta_{\bar{u}}d\tau = \zeta_{\bar{u}}(K_1\alpha + K_2)^{-1}(I - e^{-(K_1\alpha+K_2)t}) \leq (K_1\alpha + K_2)^{-1}[\lambda_{\max}(K_1)(B_{ov} + \frac{\alpha}{1+\beta'}) + \alpha]$$

In virtue of Lemma 1, when tuning gains α, K_1 and K_2 meet the condition (36), we can easily conclude that $\|\chi(t)\| \leq 1$, which confirms the boundedness of $\chi(t)$.

A.5 Proof of lower bound of g_{1i} at the condition (A25)

Introduce a function

$$f(\alpha) = \frac{1}{2\alpha\underline{m}} + \overline{m}[\frac{\alpha}{1+\beta'}S + \alpha^2 + (\frac{\alpha}{1+\beta'} + \alpha)^2]$$

whose partial derivative with respect to α are denoted by $f'(\alpha)$ and $f''(\alpha)$, given by

$$f'(\alpha) = -\frac{1}{2\alpha^2\underline{m}} + \overline{m}[\frac{10 + 12\beta' + 4\beta'^2}{1 + 2\beta' + \beta'^2}\alpha + \frac{1}{1+\beta'}S], \quad f''(\alpha) = \frac{1}{\alpha^3\underline{m}} + \overline{m}\frac{10 + 12\beta' + 4\beta'^2}{1 + 2\beta' + \beta'^2}$$

It's easy to know $f''(\alpha) > 0$ for all α satisfy condition (33). Hence, $f'(\alpha)$ is monotonically increasing with respect to α. Considering the fact $f'(0^+) < 0$ and the following equation

$$f'(\alpha)|_{\alpha=(5+5\beta')/4} = -\frac{8}{25(1+\beta')^2\underline{m}} + \overline{m}\frac{50 + 60\beta' + 20\beta'^2 + S}{1+\beta'}$$

It's worth noting that $f'((5 + 5\beta')/4) > 0$ can be satisfied in a general robotic manipulator system with constants β', $\underline{m}$ and $\overline{m}$. Therefore, the minimum value of $f(\alpha)$ can be approached as α trends to $((5 + 5\beta')/4)^+$, which denotes the right limit of point $\alpha = (5 + 5\beta')/4$, i.e.

$$\inf_\alpha f(\alpha) = \lim_{\alpha\to((5+5\beta')/4)^+} f(\alpha) = \frac{2}{5(1+\beta')\underline{m}} + \overline{m}[\frac{125}{16} + \frac{75}{8}\beta' + \frac{25}{8}\beta'^2 + \frac{5}{4}S]$$

In terms of (A24), one can know that the minimum point of the lower bound of $g_{1i}(\alpha)$ is the same as the minimum point of $f(\alpha)$, which is a sufficient conclusion. And we have completed the proof.

References

1. Kim YH, Lewis FL. Neural network output feedback control of robot manipulators. *IEEE Transactions on Robotics and Automation* 1999; 15(2): 301-309.
2. Cui R, Chen L, Yang C, Chen M. Extended State Observer-Based Integral Sliding Mode Control for an Underwater Robot With Unknown Disturbances and Uncertain Nonlinearities. *IEEE Transactions on Industrial Electronics* 2017; 64(8): 6785-6795.
3. Arimoto S, Liu YH, Naniwa T. Model-based adaptive hybrid control for geometrically constrained robots. In: ; 1993: 618-623 vol.1.
4. Aguinaga-Ruiz E, Zavala-Rio A, Santibanez V, Reyes F. Global Trajectory Tracking Through Static Feedback for Robot Manipulators With Bounded Inputs. *IEEE Transactions on Control Systems Technology* 2009; 17(4): 934-944.
5. Yin Z, Qian H, Xiao A, Wu J, Liu G. The Application of Adaptive PID Control in the Spray Robot. In: . 1. ; 2011: 528-531.
6. Sun T, Cheng L, Wang W, Pan Y. Semiglobal exponential control of Euler–Lagrange systems using a sliding-mode disturbance observer. *Automatica* 2020; 112: 108677.
7. Kardos J. Robust Computed Torque Method of Robot Tracking Control. In: ; 2019: 102-107.
8. Baek S, Baek J, Kwon W, Han S. An Adaptive Model Uncertainty Estimator Using Delayed State-Based Model-Free Control and Its Application to Robot Manipulators. *IEEE/ASME Transactions on Mechatronics* 2022; 27(6): 4573-4584.
9. Wai RJ, Chuang KL, Lee JD. On-Line Supervisory Control Design for Maglev Transportation System via Total Sliding-Mode Approach and Particle Swarm Optimization. *IEEE Transactions on Automatic Control* 2010; 55(7): 1544-1559.
10. Lewis FL, Yesildirak A, Jagannathan S. *Neural Network Control of Robot Manipulators and Nonlinear Systems*. USA: Taylor and Francis, Inc. . 1998.
11. Zhang D, Kong L, Zhang S, Li Q, Fu Q. Neural networks-based fixed-time control for a robot with uncertainties and input deadzone. *Neurocomputing* 2020; 390: 139 - 147.
12. Chen M, Ge SS. Adaptive Neural Output Feedback Control of Uncertain Nonlinear Systems With Unknown Hysteresis Using Disturbance Observer. *IEEE Transactions on Industrial Electronics* 2015; 62(12): 7706-7716.
13. Patan K, Patan M. Neural-network-based iterative learning control of nonlinear systems. *ISA Transactions* 2020; 98: 445 - 453.
14. Chen S, Wen JT. Adaptive Neural Trajectory Tracking Control for Flexible-Joint Robots with Online Learning. In: ; 2020: 2358-2364.
15. Ti-Chung Lee , Kai-Tai Song , Ching-Hung Lee , Ching-Cheng Teng . Tracking control of unicycle-modeled mobile robots using a saturation feedback controller. *IEEE Transactions on Control Systems Technology* 2001; 9(2): 305-318.
16. Meng T, He W. Iterative Learning Control of a Robotic Arm Experiment Platform with Input Constraint. *IEEE Transactions on Industrial Electronics* 2018; 65(1): 664-672.
17. Jabbari Asl H, Narikiyo T, Kawanishi M. Neural network-based bounded control of robotic exoskeletons without velocity measurements. *Control Engineering Practice* 2018; 80: 94 - 104.
18. Shojaei K, Chatraei A. A Saturating Extension of an Output Feedback Controller for Internally Damped Euler-Lagrange Systems. *Asian Journal of Control* 2015; 17(6): 2175-2187.
19. Pliego-Jiménez J, Arteaga-Pérez M, Sánchez-Sánchez P. Dexterous robotic manipulation via a dynamic sliding mode force/position control with bounded inputs. *IET Control Theory & Applications* 2019; 13(6): 832-840.
20. Aguinaga-Ruiz E, Zavala-Rio A, Santibanez V, Reyes F. Global trajectory tracking through static feedback for robot manipulators with input saturations. In: ; 2008: 3516-3522.

21. Elhaki O, Shojaei K, Mohammadzadeh A, Rathinasamy S. Robust amplitude-limited interval type-3 neuro-fuzzy controller for robot manipulators with prescribed performance by output feedback. *Neural Comput & Applic* 2023; 35(12): 9115–9130.

22. Rascón R, Moreno-Valenzuela J. Output feedback controller for trajectory tracking of robot manipulators without velocity measurements nor observers. *IET Control Theory & Applications* 2020; 14(14): 1819-1827.

23. Bouakrif F. Trajectory tracking control using velocity observer and disturbances observer for uncertain robot manipulators without tachometers. *Meccanica* 2016; 52.

24. Saab SS, Ghanem P. A Multivariable Stochastic Tracking Controller for Robot Manipulators Without Joint Velocities. *IEEE Transactions on Automatic Control* 2018; 63(8): 2481-2495.

25. Liu SB, Giusti A, Althoff M. Velocity Estimation of Robot Manipulators: An Experimental Comparison. *IEEE Open Journal of Control Systems* 2023; 2: 1-11.

26. Berghuis H, Nijmeijer H. A passivity approach to controller-observer design for robots. *IEEE transactions on robotics and automation* 1993; 9(6): 740–754.

27. Yao Q. Adaptive trajectory tracking control of a free-flying space manipulator with guaranteed prescribed performance and actuator saturation. *Acta Astronautica* 2021; 185: 283-298.

28. Zhang H, Wang Y. Adaptive neural network control of an uncertain robotic manipulator with input constraint and external disturbance. In: ; 2021: 1302-1308.

29. Zhao ZL, Guo BZ. A Novel Extended State Observer for Output Tracking of MIMO Systems With Mismatched Uncertainty. *IEEE Transactions on Automatic Control* 2018; 63(1): 211-218.

30. Shahriari-kahkeshi M, Mahdavi M. Fuzzy Control of an Uncertain Robot Manipulator with Input Constraint. In: ; 2019: 1-6.

31. Lewis FL, Yesildirak A, Jagannathan S. *Neural Network Control of Robot Manipulators and Nonlinear Systems*. Taylor amp; Francis, Inc. . 1998.

32. Lewis FL, Yesildirak A, Jagannathan S. Neural Network Control Of Robot Manipulators And Non-Linear Systems. In: ; 1998.

33. Zhang T, Zhang A. Robust Adaptive Neural Network Finite-Time Tracking Control for Robotic Manipulators Without Velocity Measurements. *IEEE Access* 2020; 8: 126488-126495.

34. Bouakrif F. Trajectory tracking control using velocity observer and disturbances observer for uncertain robot manipulators without tachometers. *Meccanica* 2016; 52.

35. Zhao ZL, Guo BZ. A nonlinear extended state observer based on fractional power functions. *Automatica* 2017; 81: 286-296.

36. Ioannou P, Baldi S. *Robust Adaptive Control*: 1-22; 2010.

37. Ma Z, Huang P. Adaptive neural-network controller for an uncertain rigid manipulator with input saturation and full-order state constraint. *IEEE Transactions on Cybernetics* 2020.

38. Arteaga-Peréz MA, Pliego-Jiménez J, Romero JG. Experimental results on the robust and adaptive control of robot manipulators without velocity measurements. *IEEE Transactions on Control Systems Technology* 2019; 28(6): 2770–2773.

39. Haykin S. *Kalman filtering and neural networks*. John Wiley & Sons . 2004.

40. Perruquetti W, Floquet T, Moulay E. Finite-Time Observers: Application to Secure Communication. *IEEE Transactions on Automatic Control* 2008; 53(1): 356-360.

41. Patre P. *Lyapunov-based robust and adaptive control of nonlinear systems using a novel feedback structure*. University of Florida . 2009.